



**NONLINEAR FLIGHT DYNAMIC ANALYSIS  
OF BLUNT BODY ENTRY VEHICLES USING  
MULTIPLE TIME SCALES METHOD**

By

**SAAD SHAHZAD SULTAN**

**NUST201260263MRCMS64012F**

**RESEARCH CENTRE FOR MODELING AND SIMULATION  
NATIONAL UNIVERSITY OF SCIENCES AND TECHNOLOGY**

**ISLAMABAD**

**2015**

**NONLINEAR FLIGHT DYNAMIC ANALYSIS OF BLUNT BODY  
ENTRY VEHICLES USING MULTIPLE TIME SCALES  
METHOD**

A Thesis submitted to the Faculty of  
Research Centre for Modeling and Simulation,  
National University of Sciences and Technology, Islamabad

by

**Saad Shahzad Sultan**

In Partial Fulfillment of the Requirements for the Degree of  
Master of Science

in

Computational Science and Engineering

May, 2015

# NONLINEAR FLIGHT DYNAMIC ANALYSIS OF BLUNT BODY ENTRY VEHICLES USING MULTIPLE TIME SCALES METHOD

By

Saad Shahzad Sultan

A Thesis submitted to the Faculty of  
Research Centre for Modeling and Simulation,  
National University of Sciences and Technology, Islamabad

In Partial Fulfillment of the Requirements for the Degree of

Master of Science  
in  
Computational Science and Engineering

## Approved by:

Dr. Adnan Maqsood  
Assistant Professor

*Research Centre for Modeling and Simulation,  
National University of Sciences and Technology,  
Islamabad*

---

(Thesis Supervisor)

Dr. Asif Farooq  
Professor

*School of Natural Sciences,  
National University of Sciences and Technology,  
Islamabad*

---

(G.E.C. Member)

Dr. Syed Salman Shahid  
Assistant Professor

*Research Centre for Modeling and Simulation,  
National University of Sciences and Technology,  
Islamabad*

---

(G.E.C. Member)

Mr. Ammar Mushtaq  
Lecturer

*Research Centre for Modeling and Simulation,  
National University of Sciences and Technology,  
Islamabad*

---

(G.E.C. Member)

May, 2015

## **STATEMENT OF ORIGINALITY**

I hereby certify that the work embodied in this thesis is the result of original research carried out by me, and has not been submitted for a higher degree to any other University or Institution.

---

Date

---

Saad Shahzad Sultan

# **DEDICATION**

*To my Parents*

## **ACKNOWLEDGEMENTS**

First of all, I am highly grateful to Almighty Allah for enabling me to complete this thesis successfully, and for the uncountable blessings He has conferred upon me in my life. I am thankful for the courage and motivation He poured in my heart.

This work would not have been what it is today without support and encouragement from my thesis supervisor, Dr. Adnan Maqsood. Thank you so much for providing me an opportunity to work under your supervision, and for guiding me so patiently and proficiently throughout the research phase. Your role as a mentor and supervisor has been vital towards the accomplishment of this thesis.

I would also like to thank my G.E.C. members, Dr. Salman Shahid, Dr. Asif Farooq and Mr. Ammar Mushtaq; for their encouragement and assistance.

I also want to thank all the faculty and staff at RCMS specially Mrs. Nusrat Nadeem, Library In-charge RCMS, for their responsiveness and for providing a beautiful learning environment.

Special thanks to my friends, especially Muhammad Usman.

## Table of Contents

<b>Chapter 1</b>	<b>Introduction to Atmospheric Entry</b> .....	<b>11</b>
1.1	Introduction .....	11
1.2	Pakistan Space Program.....	12
1.3	Area of research .....	13
1.4	Research Objectives.....	15
1.5	Methodology .....	15
1.6	Contribution of Thesis .....	17
1.7	Organization of the Thesis.....	18
<b>Chapter 2</b>	<b>Review of Literature</b> .....	<b>20</b>
2.1	Introduction .....	20
2.2	Effects of Design and Environmental Parameters Dynamic Stability .....	20
2.3	Multiple Time Scales and Limit Cycle Oscillation .....	26
2.4	Missing Links Literature .....	27
<b>Chapter 3</b>	<b>Problem Formulation</b> .....	<b>28</b>
3.1	Introduction .....	28
3.2	Derivation of Governing Equations.....	28
3.3	Assumptions .....	29
3.4	Equations of Motion .....	30
3.5	Development of Parametric Governing Equations .....	31
3.6	Concluding Remarks.....	34
<b>Chapter 4</b>	<b>Application of Multiple Time Scales Method</b> .....	<b>35</b>
4.1	Introduction to Multiple Time Scales Method.....	35
4.2	Application of MTS Method.....	37
4.3	Limit Cycle Analysis .....	39

4.4	Bifurcation Analysis .....	39
4.5	Solution of Amplitude and Phase-Correction Equation.....	42
4.6	Concluding Remarks.....	43
<b>Chapter 5</b>	<b>Numerical Validation.....</b>	<b>44</b>
5.1	Introduction .....	44
5.2	Numerical Solution .....	44
5.3	Comparison of Analytical Solution with Numerical Simulation .....	46
5.4	Concluding Remarks.....	46
<b>Chapter 6</b>	<b>Concluding Remarks .....</b>	<b>47</b>
6.1	Introduction .....	47
6.2	Conclusion .....	47
<b>References</b>	.....	<b>48</b>
<b>Appendix A</b>	.....	<b>52</b>



## List of Figures

---

Figure 1.1	Concept evolution of shapes for atmospheric entry vehicles.....	12
Figure 1.2	The trajectory of MARS entry vehicle famously known as seven minutes of terror.....	14
Figure 1.3	Research Methodology.....	17
Figure 2.1	Moments, Forces and Axis for Orion Crew Module .....	20
Figure 2.2	Stardust Capsule, Pitch Damping Coefficient for Different CG Locations at M=2 .....	21
Figure 2.3	Bluntness Effects.....	22
Figure 2.4	Forebody Roughness Effects .....	23
Figure 2.5	Aftbody Effect on Damping with Mach number on top and Angle of Attack on bottom .....	24
Figure 2.6	Simulated Oscillations, Vertical Lines Indicating Mach Number .....	25
Figure 2.7	Reynolds Number Effects for Orion and Stardust.....	25
Figure 3.1	Coordinate System.....	29
Figure 3.2	Lift Coefficient.....	32
Figure 3.3	Moment Coefficient.....	32
Figure 3.4	Damping Coefficient.....	33
Figure 4.1	Concept of Multiple Time Scales .....	36
Figure 4.2	Kinds of Limit Cycle.....	39
Figure 4.3	Bifurcation Diagram .....	40
Figure 4.4	Bifurcation Diagram .....	41
Figure 5.1	Comparison of Analytical and Numerical Solution for the LC Case.....	46

## SUMMARY

Atmospheric entry is a critical phase for mission that seeks to return astronauts or scientific payloads back to Earth or explore the surface of a planet with an appreciable atmosphere. This project aims at the comprehensive investigation of the dynamic stability of blunt body atmospheric entry vehicles. As blunt vehicle enters a planetary atmosphere, the aerodynamic moments acting upon it can result in unstable pitching motions and divergence of oscillation amplitude. Typically, these instabilities are found in the low or mid supersonic regime of the trajectory just prior to parachute deployment. The amplitude envelope of a planetary probe as it enters an atmosphere can play an important role in terminal events like the deployment of parachutes and entry/reentry trajectories. Most analysis considers the case of constant or linear aerodynamic coefficients. In many cases the aerodynamic coefficients exhibit nonlinear behavior. In this research, the nonlinearities of various stability coefficients are correlated with the system response by generating approximate closed form analytical solutions. For this purpose, the Multiple Time Scales method in conjunction with bifurcation theory is used to obtain the approximate solutions of the multiple degree-of-freedom nonlinear equations of motion. The explicit analytical results obtained are useful to identify the key parameters affecting the dynamics and stability of the blunt body atmospheric entry vehicle. The conditions leading to limit cycle responses in the vicinity of loss of damping regime are discussed. The analytical solution is duly validated with the numerical solution in the end. Such research endeavors will help the Government of Pakistan to realize the goals of “Space Programme 2040” and bring the benefits of the complete spectrum of space technology to the people of Pakistan.

## Chapter 1

# INTRODUCTION

---

## 1.1 Background

Space exploration was an impetus of scientific and technological growth during last century. It is envisioned that this century will see human landing on Martian soil. For this purpose, an atmospheric entry vehicle with human-on-board will be used to enter Martian atmosphere. Atmospheric entries are of critical standing for the missions which aim to bring scientific payloads from space to the planets with appreciable atmospheres.

The design of atmospheric entry vehicles have evolved over the years. In 1953 Allen and Eggers [1] from National Advisory Committee of Aeronautics (NACA) proposed that the blunt nose made the most effective heat shield as shown in Figure 1.1. Blunt bodies protect the vehicle from heating and play an important role in landing and reentering the atmosphere. In this discovery, it was shown that the drag coefficient is inversely proportional to the heat load experienced by the blunt body vehicles. The blunt nose forces the oblique shock waves to detach from the nose and form a curved shock wave distant from the vehicle. Since, majority of the hot gases does not directly influence the vehicle; the total heat energy will not cross the shock wave and simply deviate in surrounding of the vehicle and later will dissipate in the air.

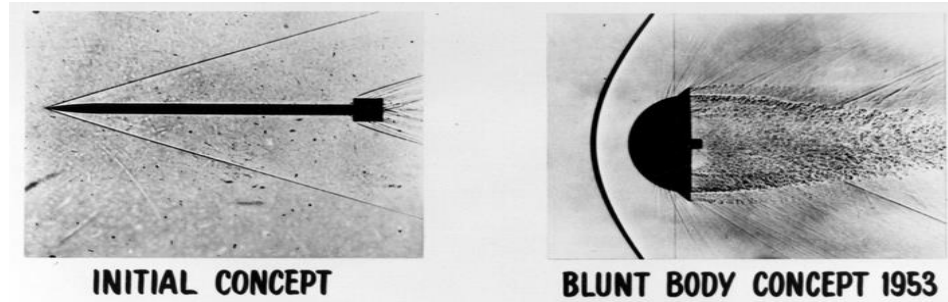


**Figure 1.1** Concept evolution of shapes for atmospheric entry vehicles [2]

During the design of atmospheric entry vehicles, it is meaningful to understand the nonlinear phenomena occurring at the time of atmospheric entry. Interestingly, the dynamic response of blunt bodies is unstable in low supersonic regimes. When a blunt entry probe enters into atmosphere of a planet, at a supersonic Mach number, undesirable self-sustained limit-cycle oscillations are born because of nonlinear aerodynamic moment acting upon it. Mostly, such instabilities came into birth due to the maximum dynamic pressure and reaches to peak in the low or mid supersonic reign of the flight trajectory, preceding to parachute opening [3]. It is critical at the time of parachute deployment that the amplitude of oscillation be less than approximately  $10^\circ$  for safe deployment [4].

## **1.2 Pakistan Space Program**

The Government of Pakistan promotes space exploration program. To synergize these efforts, Space and Upper Atmospheric Research Commission, (SUPARCO), a space exploration institute is working since 1960's. The commission is responsible to promote peaceful research in space technology and to conduct research in technology for socio-economic uplift of country. SUPARCO has achieved success in multiple projects. The first successful flight of expendable rocket, Rehbar-I [5] was recorded in 1961. Moreover, the first satellite, Badr-I was constructed by SUPARCO and launched with the cooperation of China [6].

The Government of Pakistan initiated the “Space Programme 2040” in 2011 with the aim to bring the benefits of the full spectrum of space technology to the people of Pakistan. Earlier space expeditions from Pakistan demonstrated lack-luster performance compared to other technologically advanced countries. The field of space and planetary astrophysics remained relatively obscure amongst academic disciplines taught in Pakistan, but with India’s recent launch of its Mars Orbiter Mission (MOM), the onus is now on the second-largest country in South Asia to make similar steps.

In pursuance of Space Program 2040, Pakistan will launch five GEO satellites and six LEO satellites between 2011 and 2040 [7]. The program intends to develop the military and space technologies and conduct experiments on fundamental sciences in space frontier. The research pertaining to atmospheric entry vehicles is also an integral part of space exploration program. Such research endeavors will help the Government of Pakistan to realize the goals of “Space Programme 2040”.

### **1.3 Area of Research**

Blunt body entry vehicle is an important research area. Its significance can be judged from the fact that all MARS expeditions intending to enter Martian atmosphere are blunt body entry vehicles. Once entered into Martian atmosphere, the blunt body initially reduces its velocity with the help of atmospheric resistance. Subsequently, in low supersonic regime, the drag chute is deployed to further decelerate it to subsonic speeds. In the final phase before touchdown/deployment of scientific payload, it jettisons its drag chute and becomes airborne with thrusters. Finally, the deployment of payload via sling on the Martian land culminates the mission of entry vehicle as shown in Figure 1.2.

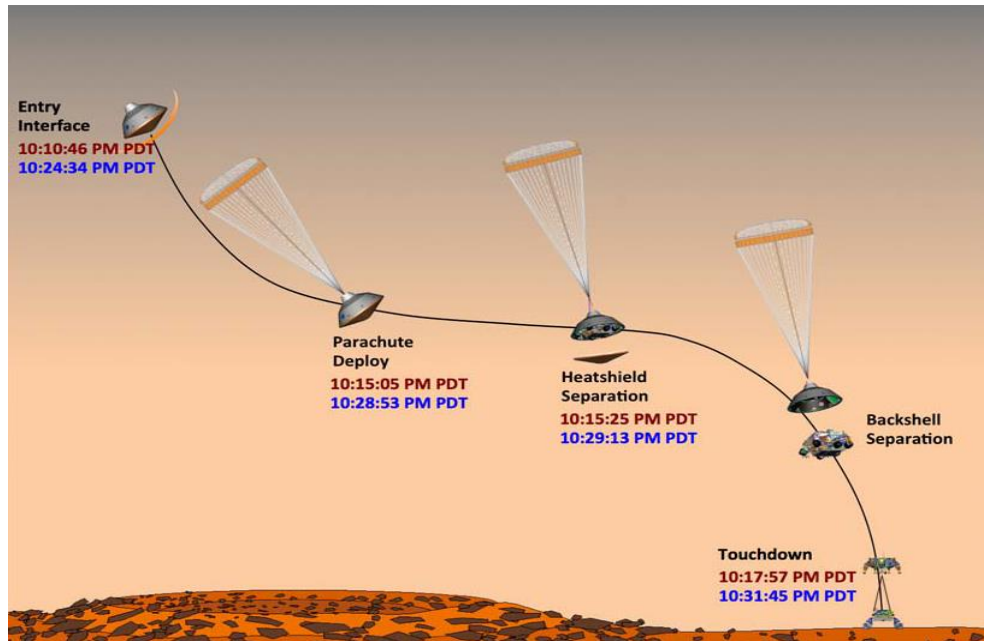


**Figure 1.2** The trajectory of MARS entry vehicle famously known as seven minutes of terror [8]

These entry vehicles are highly prone to aerodynamic instabilities. Specifically, a nonlinear dynamic phenomenon of limit-cycle oscillations is a feature of such vehicles that is studied during the design of all atmospheric entry vehicles. The limit-cycle oscillations generally emerge in low or mid supersonic regime of the trajectory just prior to parachute deployment. The cause of these oscillations is generally attributed to the development of unsteady pressure forces on the aft body of the blunt body entry vehicle. The dynamic stability is a function of vehicle design and mission trajectories. The vehicle design considerations that govern the dynamic stability are overall geometry and mass distribution. From the mission trajectory perspective, the magnitude of oscillations should be less than  $10^\circ$  where entry vehicle deploys the parachute. All these design and mission considerations are fundamentally transferred to aerodynamics and stability coefficients graphs. These graphs depict the trend of stability coefficients as a function of kinematic variables (angle of attack, pitch rate etc). The designers use these graphs to understand the dynamic behavior of atmospheric entry vehicles. However, the interactions are

generally less understood and for that purpose, designers move towards experimental, numerical or analytical approaches.

In this work, a systematic evaluation will be carried out to decipher the phenomenon of blunt body atmospheric entry vehicles dynamic stability. Analytical and numerical techniques will be used to accurately predict the dynamic response of this class of vehicles.

## **1.4 Research Objectives**

The goal of this work is to obtain an analytical solution from the planar differential equations and validate it with the numerical simulations. This work aims to fulfill the following objectives:

- Understand the dynamics of blunt-body atmospheric entry vehicles through analytical techniques
- Develop the analytical model that can relate the design aspects with the dynamic response of the vehicle
- Parameterize the equations of motion and express its solutions explicitly in terms of amplitude and frequency
- Validate the analytical solution with established numerical approach

## **1.5 Methodology**

In today's world, Modeling and Simulation (M&S) has become an intrinsic part of any engineering discipline. M&S enable the engineers to translate their creative thinking into practical designs with minimal time and less chances of error. The M&S field also circumvents actual testing and experimentation thereby cutting down the project cost in multiple folds.

Characterizing the dynamic stability performance of an entry configuration is an area of research that has been plagued with experimental difficulties, contradictory observations, and

large uncertainties. A few studies [3, 9] have tried to generate numerical predictions or generic analytical solutions. The experimental studies are either too expensive or very complex to conduct. Recently, Kazemba [10] proposed the analytical model using the time-lagged aft-body moment for limit cycle oscillations. Using these analytical solutions the effects of the boundary conditions for each setup on the equilibrium energy behavior and equilibrium oscillation amplitude were determined. The study though has shown the direction of analytical handling of such problems but lacks the integration of analytical aspects with design considerations.

The behavioral change of the stability is primarily because of the change in slope/magnitude of different static and dynamic stability curves. The static stability derivatives include pitching moment coefficient and lift coefficient variations with change in angle of attack. The dynamic stability derivatives include pitch moment damping coefficients. These coefficients can be modeled as cubic/quadratic polynomials. The coefficients of these polynomials govern the stability characteristics. In this research work, a generalized model of flight dynamic equations of motion will be generated using these polynomial coefficients. The goal is to generate an integrated model that can predict the nonlinear interaction between different coefficients.

For this purpose, the nonlinear analytical technique identified to solve this issue is known as Multiple Time Scales (MTS) method. The development of this technique is based on the work of Ramnath [11, 12]. The MTS method belongs to the family of perturbation methods. It is an asymptotic approach to approximate the physical problems that involve perturbations about nominal states specifically in limiting cases. One example is the separation of phugoid mode (slow varying manifold) and short-period mode (fast varying manifold) in aircraft longitudinal



dynamics. The MTS method is extensively used by Go [13-16] and Maqsood [17] for studying wing rock problem and UAV longitudinal dynamics respectively.

The analytical treatment from MTS analysis will be in a closed form solution. The approach will yield solutions in parametric forms and leads to the separation of fast and slow dynamics. Such solutions will have an advantage over usual numerical solutions in that the important parameters and their effects on limit-cycle characteristics, such as amplitude and frequency, can be easily seen in explicit functional relationships. The results will be duly validated with the numerical solutions in the end. The methodology adopted in this research is somewhat same as below described in Figure 1.3.

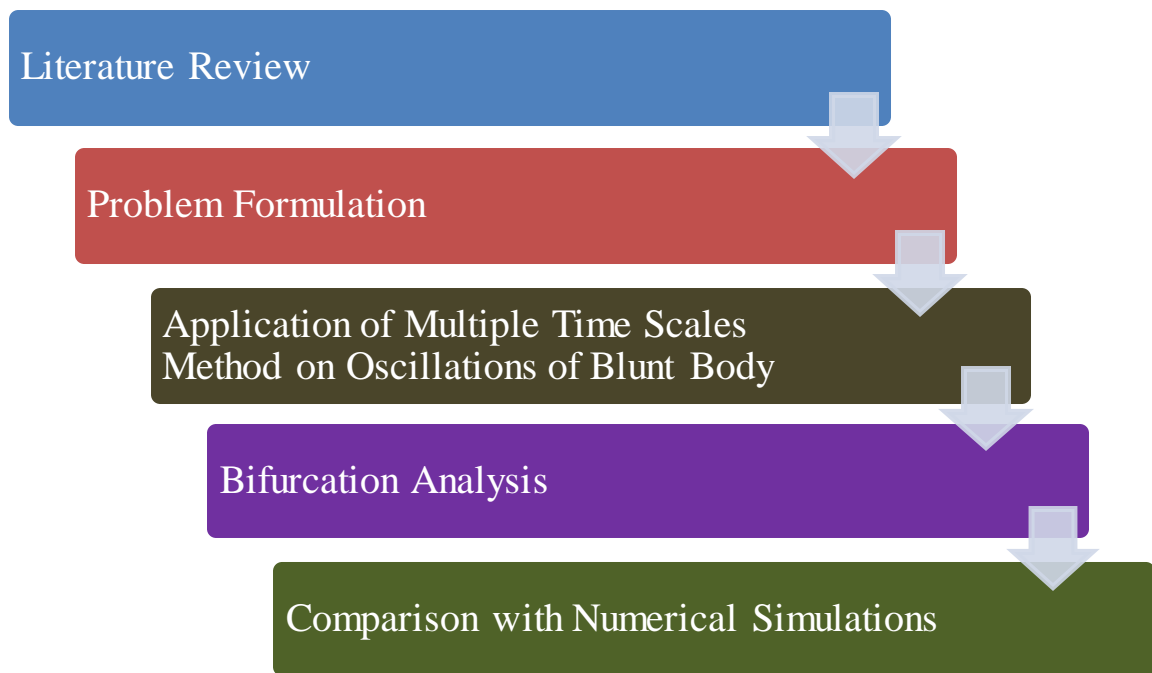


Figure 1.3 Research methodology

## 1.6 Contribution of the Thesis

During last five decades, technology protagonists investigated the flow structure around the blunt vehicle. The dynamics of a blunt body have nonlinear characteristics due to which modeling of the governing flow physics is very crucial. Most analysis had considered the case of

constant or linear aerodynamic coefficients but unfortunately atmospheric entry exhibits highly nonlinear phenomenon. The focus of this study is to use higher order polynomials for aerodynamic coefficients. In this study, the nonlinearities of various stability coefficients are correlated with the system response by generating approximately closed form solution.

This work extends the usage of analytical methods to solve the planar differential equations. Analytical method is used to study the oscillations of the blunt entry vehicle. The approach utilizes Multiple Time Scales (MTS) technique in conjunction with bifurcation theory to find the approximate solution of nonlinear differential equation.

## **1.7 Organization of the Thesis**

This thesis document has six (06) chapters. A brief description of each chapter is presented below:

### *1.7.1 Chapter 1 – Introduction*

This is the starting chapter of thesis. It gives the summary of background, problem physics, area of interest, objectives and methodology of the research.

### *1.7.2 Chapter 2 – Literature Review*

This chapter presents brief summary of the literature studies. Moreover, the effects of design and environmental parameters on the dynamic stability are also presented.

### *1.7.3 Chapter 3 – Problem Formulation*

Starting from planar model, establishment of governing equation is presented.

### *1.7.4 Chapter 4 – Application of Multiple Time Scales Analysis*

In this chapter Multiple Time Scales (MTS) technique is applied on the second order ordinary differential equation. Bifurcation analysis is also employed for the stability

characterization. Closed-form solution is obtained for the oscillations of atmospheric entry probe.

### *1.7.5 Chapter 5 – Numerical Validation*

This chapter focuses on the numerical solution obtained from the application of fourth order Runge-Kutta method. The comparison of numerical and analytical solutions are also presented.

### *1.7.6 Chapter 6 – Conclusions and Future Work*

This chapter documents crux of findings as well as chalk potential directions of future research endeavors.

## Chapter 2

# REVIEW OF LITERATURE

---

## 2.1 Introduction

In this chapter, a comprehensive review of available literature is done to understand the underlying physics of the subject problem. A brief literature survey is done in two stages. In the first stage, an understanding is developed towards the dynamic stability characteristics. The second stage focuses on the study Multiple Time Scales technique.

## 2.2 Effects of Design and Environmental Parameters on Dynamic Stability

The remarkable study of Bibb et al. [18] described the development of Orion Crew Module. They examined the uncertainties associated with the module for Mach number less than eight. The database for the aerodynamic coefficients was obtained from the wind tunnel data and the numerical simulations. The geometry of the Orion crew module is shown in Figure 2.1

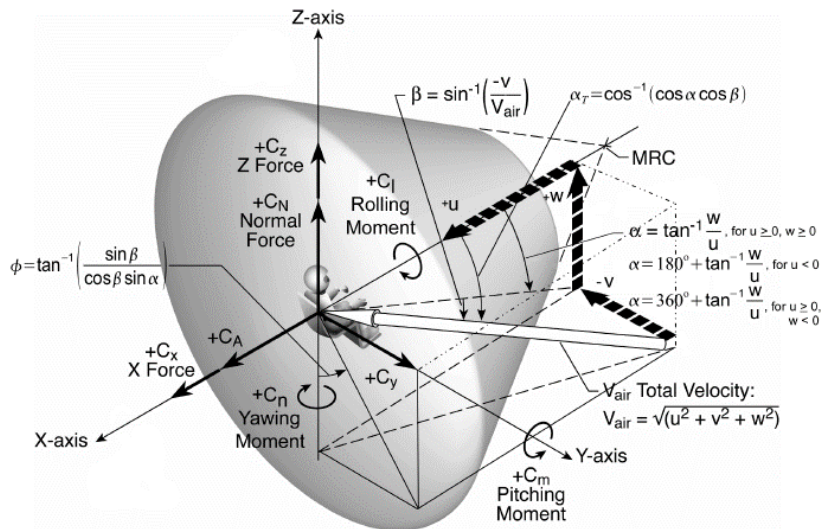


Figure 2.1 Moments, forces and axis for Orion crew module [18]

In the past half century the aerodynamic analysis was analyzed for the blunt shapes. It has become clear that the blunt body dynamic stability is highly prone to design and environmental parameters. The effects of design and environmental parameters are discussed as:

### 2.2.1 Effects of Center of Gravity Location and Roll Rate

By changing the location of CG, the dynamic stability can also be varied. Study conducted in the past have analyzed that improvement is seen in damping as the center of gravity which is shifted towards the nose. In [19] and [20], it was examined that damping improve at low angles of attack by moving the CG forward and moving rearward CG may improve damping at higher angles of attack (Figure. 2.2).

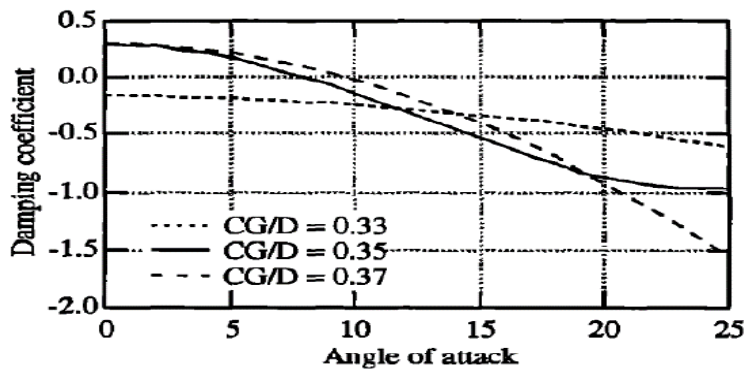


Figure. 2.2 Stardust capsule, pitch damping coefficient for different CG locations at M=2 [19]

In literature the considerable need of dynamic response of blunt probe was effected by the roll rate. Static stability can be improved in pitch and yaw directions by introducing a roll motion on a blunt probe at the time of entry. Jaffe [21] performed drop test, his results suggested that damping would increase as roll rate increases.

### 2.2.2 Effects of Forebody Cone Angle and Nose Radius

In the literature, the effect of forebody cone angle on dynamic stability demonstrates contradictory results. Most of the researchers seems to believe that the dynamic stability can be

improved by decreasing cone angle. Fletcher [22, 23] performed experimental investigations found contradictory results, related to the effects of geometric parameter variation on dynamic stability.

The great work of Allen and Eagers [1] proposed that to protect the vehicle from heating it requires to be blunt. Fletcher [22] studies are compiled in Figure 2...



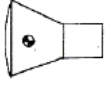
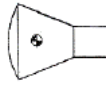
Study	Larger Nose Radius Configuration	Smaller Nose Radius Configuration
Fletcher		
Fletcher		

Figure 2.3 Bluntness effects [22], [23]

It seems to be that the slender body will be more dynamically stable. However, Ericsson [24] presented contradictory results and showed that the blunt nosed cones were more stable than the sharp nose.

### 2.2.3 Effects of Shoulder Geometry and Boundary Layer Strips

The body with sharp corners has more defined bow shock flow features relative to the body with rounded shoulder. The body with slender shoulder gives a discontinuity that will provide a fixed separation point as the flow accelerates over the body. Teramoto [25] deciphered that for the steady flow field, the recompression shock become strong due to pressure, thereby recirculation region may experience larger pressure fluctuations due to interaction between the base flow and recompression shock wave.

Wiley [26] and Ericsson [27] investigated the use of sharp shoulder geometry to establish a fixed separation point and to trip the boundary layer roughness strips on the fore-body. In Figure 2.4, the effect of roughness strip found in transonic speed is shown for a vehicle with sphere cone. It can be observed that at subsonic speeds, the roughness strip terribly reduces the dynamic stability. However, above Mach=1.1, it is seen that the stability is improved with the inclusion of roughness strip.

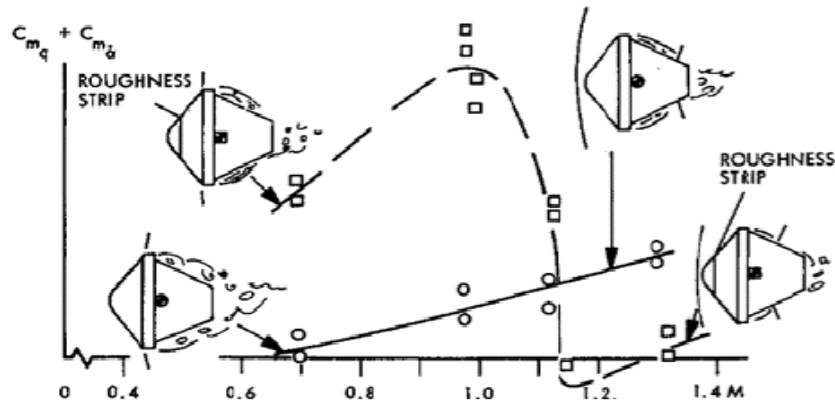


Figure 2.4 Forebody roughness effects [27]

The vehicle experiences the separation and reattachment at supersonic speeds. The effect of the reattachment occurs further aft for the smooth body having larger moment due to the unsteady pressure forces and results in reduced dynamic stability, relative to roughness strip of the body [28].

#### 2.2.4 Aftbody Effects

In the past studies of the blunt body dynamics, researchers have noticed that the aftbody geometry of the vehicle affects the stability characteristics. The presence of aftbody decreases damping for all Mach numbers with the effect being more pronounced at lower Mach numbers for the parabolic body and consistent across all Mach numbers for the sphere cone with the small aftbody.

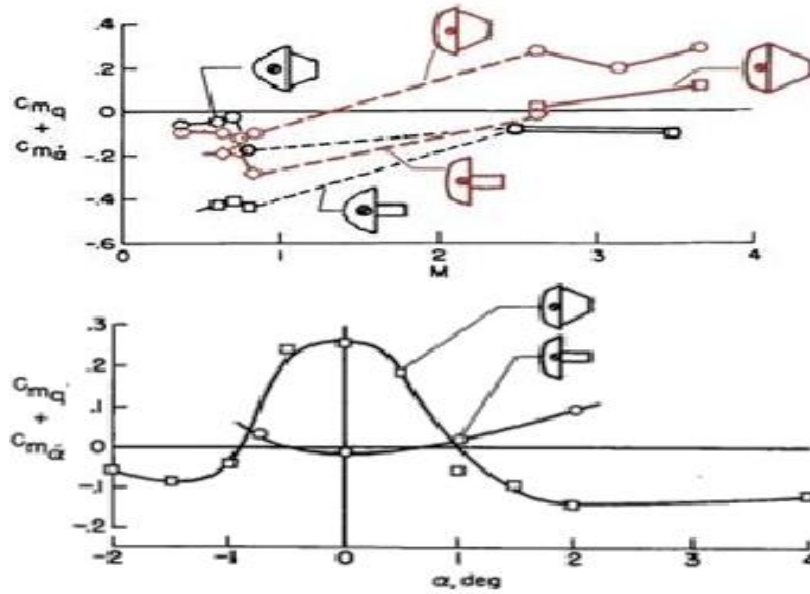


Figure 2.5 Aftbody effect on damping with Mach number on top and angle of attack on bottom [29], [30]

From Figure 2.5, it can be seen that with increase in angle-of-attack the vehicle with the aftbody becomes stable. The study in the aftbody flare by Fletcher and Wolhart [22] reveals that the addition of flare to vehicle somewhat decreased dynamic stability.

### 2.2.5 Mach Number

In hypersonic regime, damping increases favorably with Mach number. Loss of damping characteristics is observed between hypersonic and subsonic regimes. The onset of unstable mode generally appears from Mach 3 and lasts sonic conditions as shown in Figure 2.6. In subsonic regime, however, the blunt body regains damped behavior and fosters dynamically stable modes. Such a behavior results in an oscillatory envelope history that gradually starts converging towards zero from atmospheric integrate to high supersonic Mach numbers, after that it starts to grow promptly before it converges again subsonically through the transonic regime.



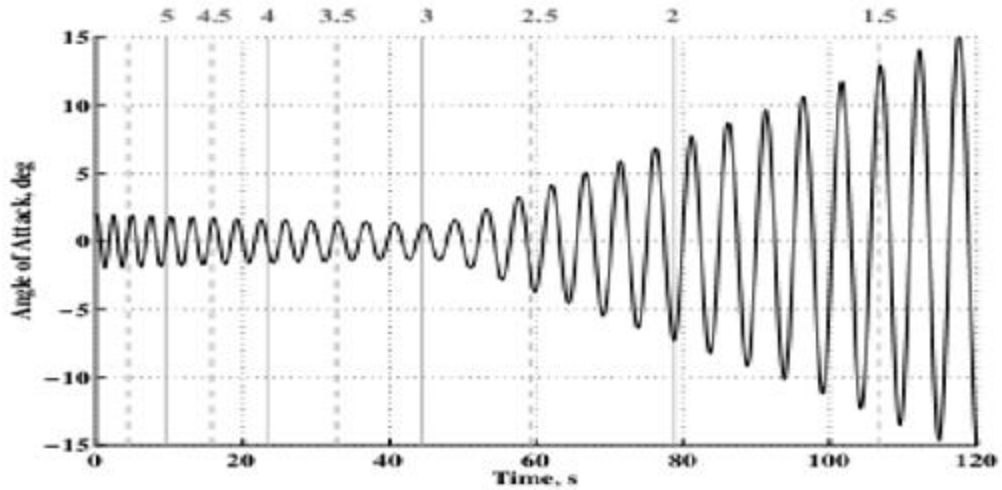


Figure 2.6 Simulated oscillations, vertical lines indicating Mach number [31]

### 2.2.9 Reynolds Number

The effect of Reynolds number is reported but with unconvincing and contradictory results. In Figure 2.7, results from Stardust [32] and Orion [33] were taken. It is seen that, with the change in Reynolds number the location and the degree of flow separation as well as the characteristics of the boundary and shear layers change and thereby variation in associated damping characteristics also occur.

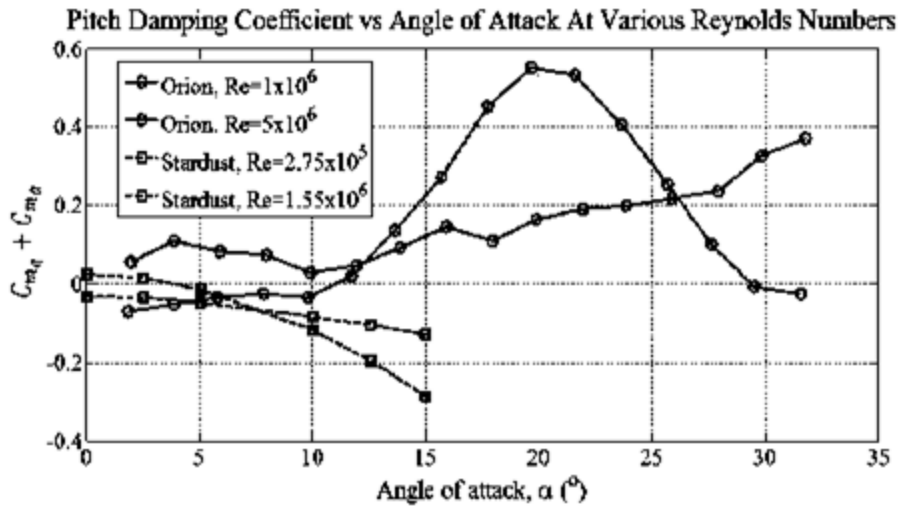


Figure 2.7 Reynolds number effects for Orion [33] and Stardust [32]

### **2.3 Multiple Time Scales (MTS) Method and Limit Cycle Oscillations**

Blunt body atmospheric entry vehicles exhibit nonlinear behavior. The behavior manifests itself as self-sustained oscillations also known as Limit Cycle Oscillations (LCOs). The analytical modeling of LCOs is generally carried out through perturbation techniques.

In this research, Multiple Time Scales (MTS) method, a class of perturbation techniques is used to develop approximate closed-form analytical solution from governing flight dynamic equations of motion. Nayfeh [34-37] explained the fundamentals and presented multiple dynamic problems through this technique. Ramnath [38] gave the basics and limitations of this technique and proposed generalized MTS method. Ramnath and Go [39] applied MTS along with bifurcation analysis to obtain analytical solution of aircraft wing rock dynamics.

Chapman and Yates [19] presented a study of limit cycle analysis, applied to blunt body aerodynamics. Planar model is used in the development of governing equations. Third order polynomials are used for aerodynamic coefficient to develop the analytical solution of amplitude of the limit cycle. However, the coefficients of third order polynomials were equated to zero. By doing this, the problem was reduced to linear approximation.

Schoenenbeger and Queen [9] presented an overview to help the researchers to understand influence of different forces and nonlinear pitching moments acting on blunt vehicles which result in limit cycle motions. Dynamic wind tunnel testing is used to measure the aerodynamic coefficients. In a vertical spin tunnel, terminal velocity is measured, dynamically scaled model of vehicle is used to obtain dynamics alike as flight conditions. Due to extreme variations in drag, manipulation of the freestream velocity is required to balance the drag with model weight.

## **2.4 Missing Links in Literature**

The complex phenomenon behind the atmospheric entry of blunt probe is not fully discussed in literature. The dynamic stability characteristic of blunt entry vehicle is one of the less understood phenomenon. Experimental and computational techniques are presented extensively in literature but analytical treatment of the instabilities occurring at the time of entry is not dealt in detail. The atmospheric entry of blunt probe as modeled by the Planar Model has not yet been addressed by MTS method. Moreover, in literature, only first or second order polynomials were used for aerodynamic coefficients whereas in this work third order polynomials are employed to grasp the underlying dynamical phenomena.

## Chapter 3

# PROBLEM FORMULATION

---

### 3.1 Introduction

In this chapter governing equations are developed using planar model. Second order ordinary differential equations are used to model the dynamic system. By taking some appropriate assumptions a nonlinear differential equation is developed. In previous studies constant and second order polynomials are used. In this study third order polynomials are used for lift and moment coefficients and second order polynomial is used for damping coefficient. By this improvement the nonlinearities present in the system can be analyzed more accurately. These polynomials are obtained from different studies with the help of graph digitizer.

### 3.2 Derivation of Governing Equations

Consider the planar differential equations of motion for a body flying in a gravity field over a spherical, non-rotating planet. Equation (3.1) to Equation (3.3) [9] describe the planar motions. Equation (3.1) is describing the sum of all the forces acting on a body in the direction of motion. Equation (3.2) represents the change in flight path angle ' $\gamma$ ' due to forces normal to the direction of motion, gravity and centrifugal forces. These equations are valid at angles-of-attack less than  $30^\circ$  for blunt shapes [9]. The coordinate system for the planar differential Equation (3.1) through Equation (3.3) is shown in Figure 3.1.

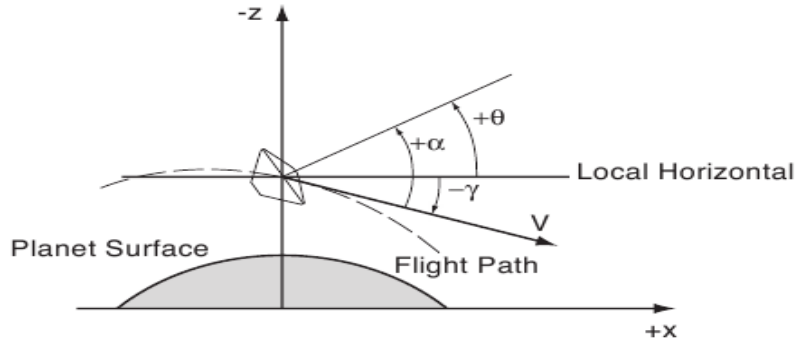


Figure 3.1 Coordinate system [9]

$$\dot{V} = -\frac{\rho V^2 S C_d}{2m} - g \sin \gamma_0 \quad (3.1)$$

$$\dot{\gamma} = \frac{\rho V S C_l}{2m} - \left(\frac{g}{V} - \frac{V}{R}\right) \cos \gamma_0 \quad (3.2)$$

$$\ddot{\theta} = \frac{\rho V^2 S d}{2I} \left( C_{m_q} \frac{\dot{\theta} d}{2V} + C_{m_{\dot{\alpha}}} \frac{\dot{\alpha} d}{2V} + C_{m_{\alpha}} \alpha \right) \quad (3.3)$$

Relative to the mean local flight path angle, the angular orientation can be defined as,

$$\theta = \alpha + \gamma \quad (3.4)$$

where  $m$  is mass of the vehicle,  $\rho$  is the density of air,  $I$  is the vehicle inertial moment about the pitch axes,  $g$  is gravity,  $S$  is a surface area of vehicle,  $V$  is the velocity,  $R$  is the radius of the planet, and  $C_d, C_l, C_m, C_{m_q}$  and  $C_{m_{\dot{\alpha}}}$  are drag, lift, moment, pitch damping and damping due to plunging coefficients which are nonlinear in angle-of-attack,  $\alpha$ .

### 3.3 Assumptions

The simplifying assumptions must be kept in mind before proceeding to the derivation of the model description of the motion.

- (i) Motions should be restricted to a plane
- (ii) Body have small lift-to-drag ratio
- (iii) Angle-of-attack is less than  $30^\circ$
- (iv) Constant acceleration due to gravity field

- (v) Spherical and non-rotating planet
- (vi) Mass of vehicle remain constant
- (vii) No effects of cross winds or atmospheric winds
- (viii) Contribution of gravitational and centrifugal forces are negligible

### 3.4 Equations of Motion

Based on aforesaid assumptions, RHS of Equation (3.2) is simplified to only contribution due to lift. Flight path angle variation due to lift coefficient is only valid for ballistic range flights, spin tunnel flight and some wind tunnel testing with free to oscillate condition. Using these assumptions, first and second derivatives of Equation (3.2) and Equation (3.4) can be taken. Using Equation (3.1) in Equation (3.2), also neglecting  $\gamma_0$  term in Equation (3.2) and then finally using these derivatives, expressing Equation (3.3) only in terms of angle of attack,

$$\ddot{\alpha} + \left(\frac{\rho VS}{2m}\right)^2 C_d C_{l_\alpha} \alpha + \frac{\rho VS}{2m} C_{l_\alpha} \dot{\alpha} = \frac{\rho V^2 S d}{2I} \left( C_{m_q} \frac{\dot{\theta} d}{2V} + C_{m_{\dot{\alpha}}} \frac{\dot{\alpha} d}{2V} + C_{m_\alpha} \alpha \right) \quad (3.5)$$

The second term on the LHS of the Equation (3.4) is small in present case and can be neglected. The first term on the RHS of the Equation (3.5) can be expressed in terms of  $\dot{\gamma}$  and  $\dot{\alpha}$ . Therefore it becomes,

$$C_{m_q} \frac{\dot{\theta} d}{2V} = C_{m_q} \left( \frac{\dot{\theta} d}{2V} + \frac{\rho S d C_l}{4m} \right) \quad (3.6)$$

Now, the second term on the RHS of the Equation (3.6) can be neglected, because

$\frac{\rho S d}{4m} C_L$  is small compared to the  $\dot{\alpha}$  term. In Equation (3.5) the terms associated with Drag

Coefficient are very small, can be neglected in the present case.

$$\ddot{\alpha} - \frac{\rho VS}{2m} \left( -C_{l_\alpha} + \frac{m d^2}{2I} (C_{m_q} + C_{m_{\dot{\alpha}}}) \right) \dot{\alpha} - \frac{\rho V^2 S d}{2I} C_{m_\alpha} \alpha = 0 \quad (3.7)$$

Several studies [3,9] have used this equation for the starting point for the analysis. After applying further conditions for each of the technique that changes form of the equation. To obtain analytical solution of Equation (3.7), the density and aerodynamic coefficients are held constant. But the case presented here is not considering constant aerodynamic coefficients. In this lift and pitching moment coefficients are expanded through third order polynomials and damping.

### 3.5 Development of Parametric Governing Equations

The aerodynamic data used in this work is taken from different papers. In Pakistan there is no facility of wind tunnel testing or any experimental testing. With the help of ‘GetData’ Graph Digitizer software data is extracted from the plots of experimental testing of blunt probes.

#### 3.5.1 Lift Coefficient

Here the data used for the lift coefficient is taken from the remarkable work of Karen et al. [18]. Their work on the development of Crew Module gives good understanding of atmospheric entry at supersonic speeds. For Mach number 2.5, the lift coefficient plot is of our interest. The lift coefficient after extracting data with software is shown in Figure (3.2) as shown below, dotted line in the plot is third order polynomial fitted i.e. Equation (3.8).

$$C_l = C_{l_{\alpha,0}}\alpha + C_{l_{\alpha^2}}\alpha^2 + C_{l_{\alpha^3}}\alpha^3 \quad (3.8)$$

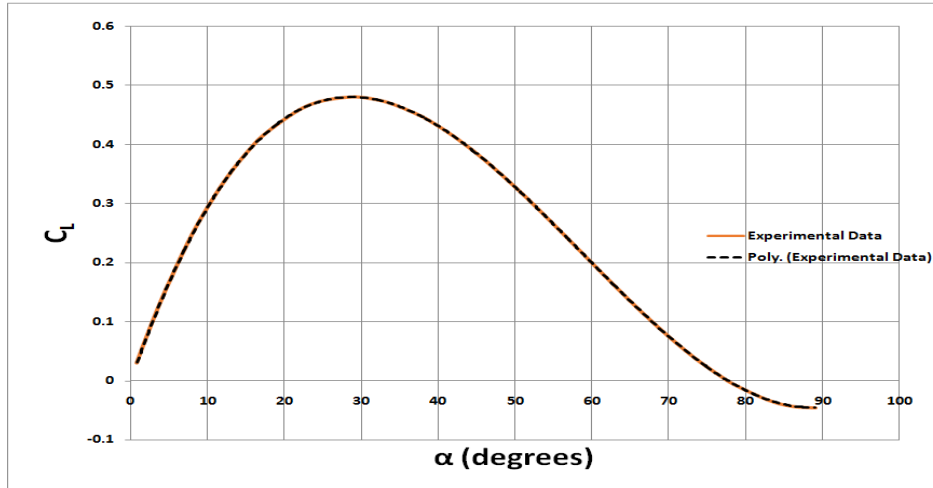


Figure 3.2 Lift coefficient [18]

### 3.5.2 Moment Coefficient

Moment coefficient plot is shown in Figure (3.9) and the data is taken from the same source , Karen et al. [18] as for the lift coefficient.

$$C_m = C_{m_{\alpha,0}} \alpha + C_{m_{\alpha^2}} \alpha^2 + C_{m_{\alpha^3}} \alpha^3 \quad (3.9)$$

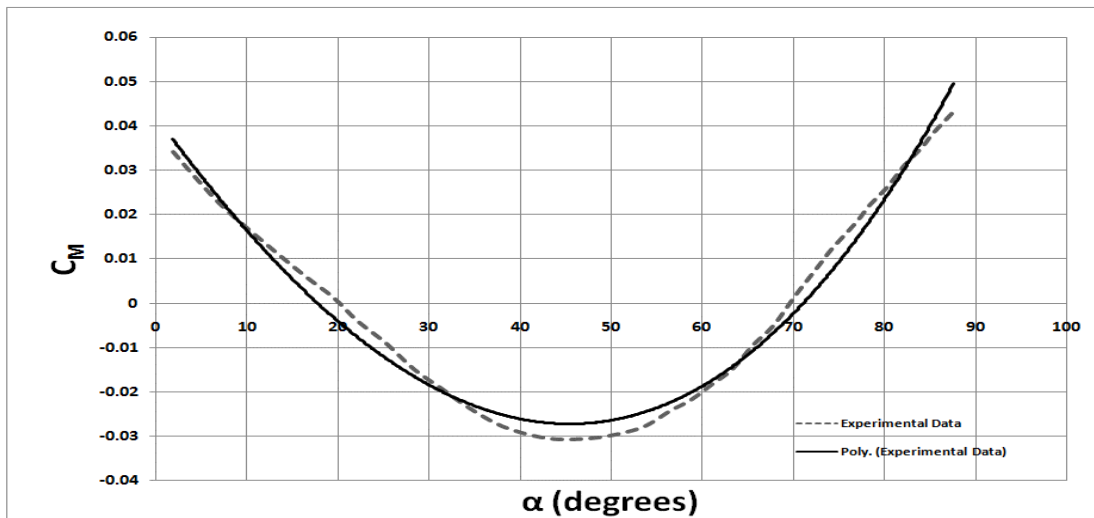


Figure 3.3 Moment coefficient [18]



### 3.5.3 Damping Coefficient

The second order polynomial for the damping coefficient is used in this work, was taken from Schoenenberger and Queen [9] remarkable work.

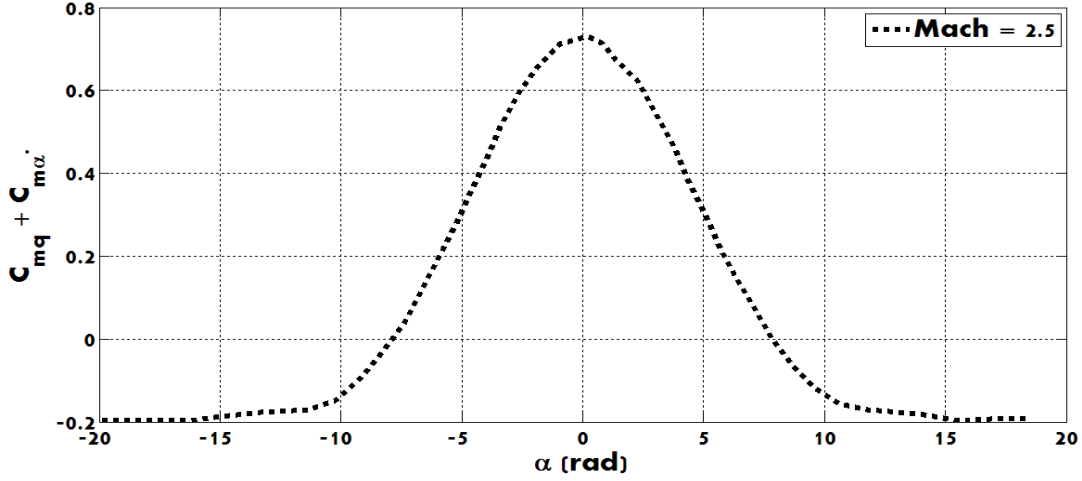


Figure 3.3 Damping coefficient [9]

$$(C_{m_q} + C_{m_{\dot{\alpha}}}) = (C_{m_q} + C_{m_{\dot{\alpha}}})_0 + (C_{m_q} + C_{m_{\dot{\alpha}}})_{\alpha} + (C_{m_q} + C_{m_{\dot{\alpha}}})_{\alpha^2} \quad (3.10)$$

Substituting the values of  $C_l, C_m$  and  $(C_{m_q} + C_{m_{\dot{\alpha}}})$  in Equation (3.5), we get;

$$\begin{aligned} \ddot{\alpha} - \frac{\rho V^2 S d}{2I} C_{m_{\alpha_0}} \alpha &= \frac{\rho V S}{2m} \left( -C_{l_{\alpha_0}} + \frac{m d^2}{2I} (C_{m_q} + C_{m_{\dot{\alpha}}})_0 \right) \dot{\alpha} + \frac{\rho V^2 S d}{I} C_{m_{\alpha^2}} \alpha^2 + \frac{3\rho V^2 S d}{2I} C_{m_{\alpha^3}} \alpha^3 + \\ \frac{\rho V S}{2m} \left( -2C_{l_{\alpha^2}} + \frac{m d^2}{2I} (C_{m_q} + C_{m_{\dot{\alpha}}})_{\alpha} \right) \alpha \dot{\alpha} &+ \frac{\rho V S}{2m} \left( -3C_{l_{\alpha^3}} + \frac{m d^2}{2I} (C_{m_q} + C_{m_{\dot{\alpha}}})_{\alpha^2} \right) \alpha^2 \dot{\alpha} \end{aligned} \quad (3.11)$$

Equation (3.11) can be written as:

$$\ddot{\alpha} + \omega^2 \alpha = \mu \dot{\alpha} + \bar{C}_1 \alpha^2 + \bar{C}_2 \alpha^3 + \bar{C}_3 \alpha \dot{\alpha} + \bar{C}_4 \alpha^2 \dot{\alpha} \quad (3.12)$$

The coefficients in Equation (3.12) are derived from the coefficients in Equation (3.11)

where  $\alpha$  and  $\dot{\alpha}$  are the pitch angle and pitch rate respectively.

$$\omega^2 = -\frac{\rho V^2 S d}{2I} C_{m_{\alpha,0}} \quad (3.13)$$

$$\mu = \frac{\rho V S}{2m} \left( -C_{l_{\alpha,0}} + \frac{m d^2}{2I} (C_{m_q} + C_{m_{\dot{\alpha}}}) \right) \quad (3.14)$$

$$C_1 = \frac{\rho V^2 S d}{I} C_{m_{\alpha^2}} \quad (3.15)$$

$$C_2 = \frac{3\rho V^2 S d}{2I} C_{m_{\alpha^3}} \quad (3.16)$$

$$C_3 = \frac{\rho V S}{2m} \left( -2C_{l_{\alpha^2}} + \frac{m d^2}{2I} (C_{m_q} + C_{m_{\dot{\alpha}}}) \right) \quad (3.17)$$

$$C_4 = \frac{\rho V S}{2m} \left( -3C_{l_{\alpha^3}} + \frac{m d^2}{2I} (C_{m_q} + C_{m_{\dot{\alpha}}}) \right) \quad (3.18)$$

### 3.6 Concluding Remarks

The derivation of Equation (3.7) is taken from Schoenenberger and Queen [9] work, started from planar model they have derived the governing Equation (3.7). Third order polynomial is used for pitching moment and lift coefficients. With this improvement Equation (3.12) is achieved. In the next chapter, further analysis will start from this equation.

## Chapter 4

# Application of Multiple Time Scales Analysis

---

### 4.1 Introduction to Multiple Time Scales Method

A vast class of complex dynamical systems exhibit phenomena that are described by a mixture of slow and fast variations. To look deeply into the behavior of such dynamical systems, a separation of slow and fast variations is helpful. The intrinsic idea behind this extension is to expand the domain of independent variable to a higher dimension space.

MTS is a powerful perturbation technique to obtain approximate solution of dynamical systems involving a mixed behavior of rapid and slow variations. This technique was developed from the work of Poincare [40] on the secular expansion in celestial mechanics. Nayfeh [34-37] has briefly studied the perturbation techniques. Ramnath [38] give a brief view of MTS technique applied to the several problems. The analytical approximation developed for the application of MTS technique in the present study is mainly based on the work of Go & Ramnath [39] and Maqsood & Go [41].

The main concept behind the MTS technique is to select the appropriate time scales depending on the behavior of the system. The quality of solution can be determined by the selection of the appropriate time scales.

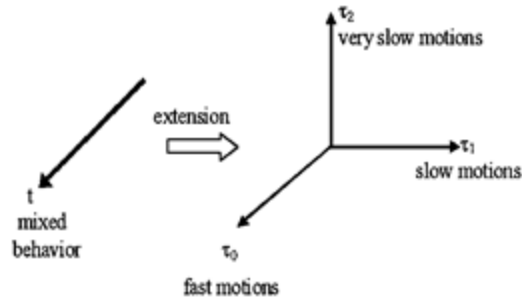


Figure 4.1 Concept of Multiple Time Scales analysis [38]

Go and Ramnath (2001) [39] applied the MTS method combining with the bifurcation theory to develop the analytical solution of the wing rock dynamics on a rigid aircraft with multiple rotational degrees-of-freedom. MTS technique was successfully applied to the two degree-of-freedom wing rock dynamics. They obtained the analytical solution which yields in parametric forms and leads to the separation of rapid and slow dynamics.

Maqsood and Go [41] have analyzed longitudinal dynamics at sustained high angle-of-attack flights observed by Unmanned Aerial Vehicle (UAV) equipped with versatile features such as aerodynamic vectoring. In their work, the derivative expansion method is used to analyze the longitudinal dynamics of UAV. Experimental data is obtained from wind tunnel testing of UAV with aerodynamic vectoring. Bifurcation theory is used to develop closed-form solution which is further validated with numerical solutions.

In this chapter, the MTS method is applied to a single degree of freedom atmospheric entry of blunt probe. Equation (3.19), highly nonlinear in  $\alpha$ , is solved by MTS perturbation technique to reach the closed-form solution. Bifurcation analysis is also carried out in this chapter to bifurcate between stable and unstable solutions.

## 4.2 Application of MTS Method

During the atmospheric entry of blunt probe, highly oscillatory behavior occurs and body starts to decelerate and aerodynamic moments acting upon it can result in unstable pitching motions and divergence of oscillation amplitude. Due to the finite convection velocity in the flow, the huge wake arises behind the forebody motion. A hysteresis effect on the pitching motion and aftbody come into birth. This will make wake structure become more complex.

Parameterizing the equation of motion i.e. Equation (3.12) as follows:

$$\ddot{\alpha} + \omega^2 \alpha = \varepsilon(\mu \dot{\alpha} + C_1 \alpha^2 + C_2 \alpha^3 + C_3 \alpha \dot{\alpha} + C_4 \alpha^2 \dot{\alpha}) \quad (4.1)$$

where,  $0 < \varepsilon \ll 1$ . Application of MTS method is now invoked to Equation (4.1). In this work, two time scales are used for the analysis. The fundamental concept behind the method is defined as:

$$t \rightarrow \{\tau_0, \tau_1\}; \quad \tau_0 = t$$

$$\tau_1 = \varepsilon t$$

$$\alpha(t) \rightarrow \alpha_0(\tau_0, \tau_1) + \varepsilon \alpha_1(\tau_0, \tau_1) + \dots$$

In above expansion,  $\tau_0$  and  $\tau_1$  represent fast and slow time scales, respectively. Then the equation of motion i.e. Equation (4.1) becomes:

$$\frac{\partial^2 \alpha_0}{\partial \tau_0^2} + \omega^2 \alpha_0 + \varepsilon \left[ \frac{\partial^2 \alpha_1}{\partial \tau_0^2} + \omega^2 \alpha_1 + 2 \frac{\partial^2 \alpha_0}{\partial \tau_0 \partial \tau_1} \right] = \varepsilon \left[ \mu \frac{\partial \alpha_0}{\partial \tau_0} + C_1 \alpha_0^2 + C_2 \alpha_0^3 + C_3 \alpha_0 \frac{\partial \alpha_0}{\partial \tau_0} + C_4 \alpha_0^2 \frac{\partial \alpha_0}{\partial \tau_0} \right] \quad (4.2)$$

The above equation only terms up to  $O(\varepsilon)$  are shown, so that these equations are appropriate to obtain both zeroth and first order approximation of the solution. Now equating the like powers of  $\varepsilon$  from Equation (4.2), we get two equations of  $O(1)$  and  $O(\varepsilon)$ .

$$O(1): \quad \frac{\partial^2 \alpha_0}{\partial \tau_0^2} + \omega^2 \alpha_0 = 0 \quad (4.3)$$

$$O(\epsilon): \frac{\partial^2 \alpha_1}{\partial \tau_0^2} + 2 \frac{\partial^2 \alpha_0}{\partial \tau_0 \partial \tau_1} = \mu \frac{\partial \alpha_0}{\partial \tau_0} + C_1 \alpha_0^2 + C_2 \alpha_0^3 + C_3 \alpha_0 \frac{\partial \alpha_0}{\partial \tau_0} + C_4 \alpha_0^2 \frac{\partial \alpha_0}{\partial \tau_0} \quad (4.4)$$

From literature [28], solution of Equation (4.3) is found as,

$$\alpha_0 = A(\tau_1) \sin \Psi \quad ; \quad \Psi = \omega \tau_0 + B(\tau_1) \quad (4.5)$$

In above equation  $\psi$  is the phase angle,  $A$  is amplitude and  $B$  is phase correction. It can be seen in the Equation (4.5), the amplitude and the phase correction of the solution vary with the slow time scale  $\tau_1$ . To find the solution of the Equation (4.4), substituting Equation (4.5) into Equation (4.4) we get:

$$\begin{aligned} \frac{\partial^2 \alpha_1}{\partial \tau_0^2} + 2\omega \frac{dA}{d\tau_1} \cos \Psi - 2\omega A \frac{dB}{d\tau_1} \sin \Psi = \mu \omega A \cos \Psi + C_1 A^2 \sin^2 \Psi + C_2 A^3 \sin^3 \Psi + \\ C_3 \omega A^2 \sin \Psi \cos \Psi + C_4 \omega A^3 \sin^2 \Psi \cos \Psi \end{aligned} \quad (4.6)$$

By using *sin* and *cos* cubic identities, and simplifying further,

$$\begin{aligned} \frac{\partial^2 \alpha_1}{\partial \tau_0^2} - C_1 A^2 \sin^2 \Psi - C_3 \omega A^2 \sin \Psi \cos \Psi = \left( -2\omega \frac{dA}{d\tau_1} + C_4 \omega \frac{A^3}{4} + \mu \omega A \right) \cos \Psi + \\ \left( 2\omega A \frac{dB}{d\tau_1} + \frac{3}{4} C_2 A^3 \right) \sin \Psi - C_4 \omega \frac{A^3}{4} \cos 3\Psi \end{aligned} \quad (4.7)$$

The terms associated with  $\cos \psi$  and  $\sin \psi$  are destroying uniformity of the solution of Equation (4.7). These terms are contributing in terms of  $\tau_0 \sin \psi$  and  $\tau_0 \cos \psi$ , which are known as secular terms that are growing without any bound with time. Results are shown in the following equation:

$$\frac{dA}{d\tau_1} = \mu \frac{A}{2} + \xi_1 A^3 \quad ; \quad \frac{dB}{d\tau_1} = \xi_2 A^2 \quad (4.8)$$

where,

$$\xi_1 = \frac{C_4}{8} = \frac{1}{8} \left( \frac{\rho V S}{2m} \left( -3C_{l_{\alpha^3}} + \frac{md^2}{2I} (C_{m_q} + C_{m_{\dot{\alpha}}})_{\alpha^2} \right) \right)$$

$$\xi_2 = -\frac{3C_2}{8\omega} = \frac{3}{8\omega} \left( \frac{3\rho V^2 S d}{2I} C_{m_{\alpha^3}} \right)$$

### 4.3 Limit Cycle Analysis

The dynamical systems having self-sustained oscillations give birth to the finite amplitude oscillations i.e. limit cycle oscillation. Mathematically, the limit cycle is a closed trajectory for which energy of the system remains constant over the cycle. Three kinds of limit cycles are shown in Figure 2.8.

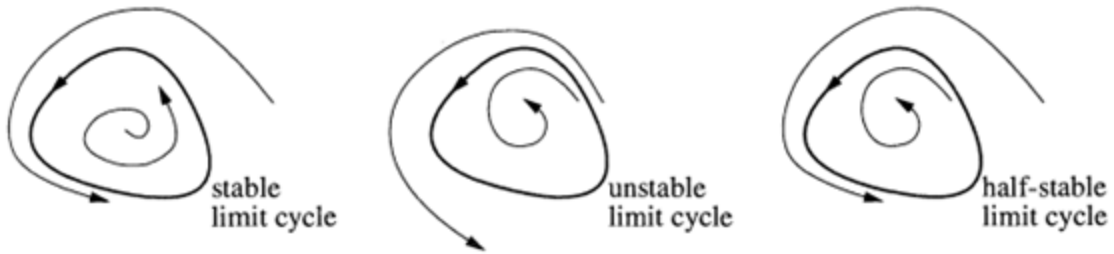


Figure 4.2 Kinds of Limit Cycle [42]

Limit cycle analysis provides aid to demonstrate the nonlinearities of pitch damping characteristics of blunt probe. For the planetary atmospheric entry, knowledge of limit cycle is significant for important affairs like parachute deployment during landing.

### 4.4 Bifurcation Analysis

Bifurcation analysis has its importance in understanding the properties of ordinary differential equations as the numerical values of some specific parameters are varied. Specifically, the stability of Equation (4.8) and changes in the topological properties of the solution can be described with help of bifurcation analysis.

The equilibria of amplitude Equation (4.8), are  $A = 0$  and  $A = \sqrt{-\frac{\mu}{2\xi_1}}$ . Plot of equilibria is shown in  $A_1 - \mu$  diagram. The stability of these equilibria is of our interest and can be determined through examining the eigenvalues of the linearized system around the equilibria of

interest. In this case, the first equilibria of interest is at  $\mu - axis$  ( $A = 0$ ). After linearization around this equilibrium, we have:

$$\frac{dA}{d\tau_1} = \mu \frac{A}{2} \quad (4.9)$$

The eigenvalue can be seen in Equation (4.9) is  $\frac{\mu}{2}$ . The sign of  $\mu$  governs the stability properties. Furthermore, the stability of second equilibrium of interest is about the parabola i.e.

$A = \sqrt{-\frac{\mu}{2\xi_1}}$ . The stability properties of these equilibria for  $\xi_1 > 0$  and  $\xi_1 < 0$  are shown in

Figure (4.3) and Figure (4.4).

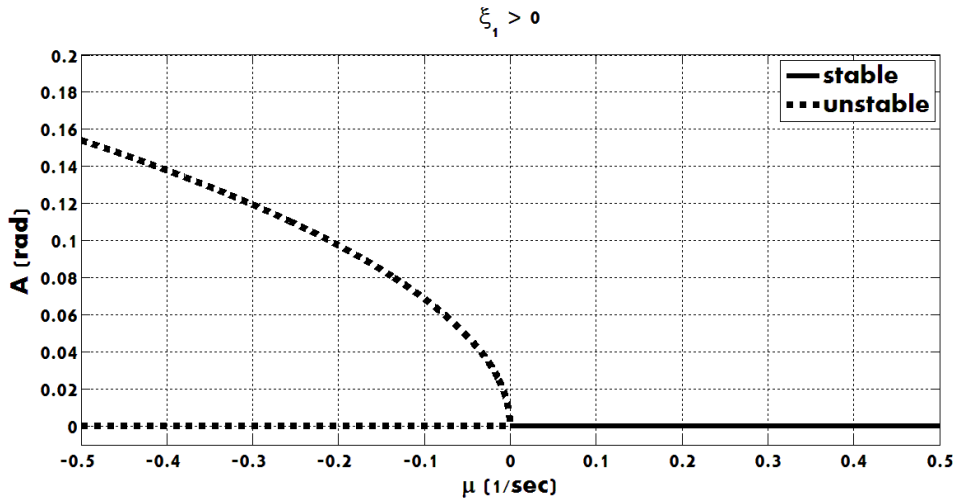


**Figure 4.3 Bifurcation Diagram for  $\xi_1 > 0$**

These bifurcation diagrams signify that there occur limit cycle (finite amplitude oscillations) appearing and disappearing in the system by varying  $\mu$  across  $\mu = 0$ . This anomaly is recognized as Hopf bifurcation. The Hopf bifurcation is subcritical for  $\xi_1 > 0$ , although for the values of  $\mu$  below the onset of bifurcation, the new branch of equilibria will occur. The Hopf bifurcation is supercritical for  $\xi_1 < 0$ , as the new branch of equilibria exist only for values of  $\mu$  larger than the bifurcation onset.



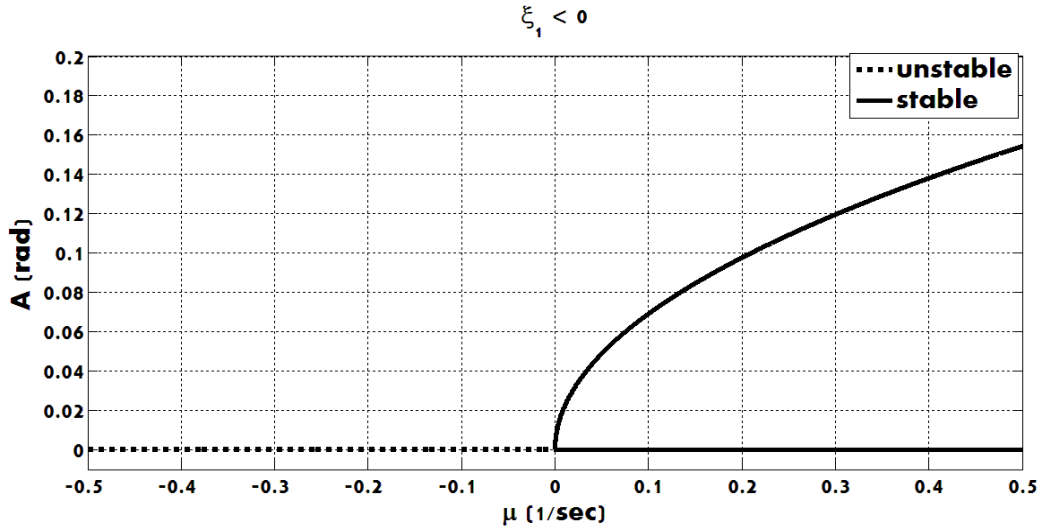


**Figure 4.4 Bifurcation diagram for  $\xi_1 < 0$**

It can be seen from the bifurcation diagram that, only for  $\xi_1 < 0$  the limit cycle is possible. This bifurcation study signifies that the sustained oscillation can only occur when  $\xi_1 < 0$  and the amplitude of limit cycle is given by:

$$A = \sqrt{-\frac{\mu}{2\xi_1}} \quad (4.10)$$

The amplitude only depends on  $\mu$  and  $\xi_1$ .

$$\mu = \frac{\rho VS}{2m} \left( -C_{l_{\alpha,0}} + \frac{md^2}{2I} (C_{m_q} + C_{m_{\dot{\alpha}}})_0 \right)$$

$$\xi_1 = \frac{1}{8} \left( \frac{\rho VS}{2m} \left( -3C_{l_{\alpha^3}} + \frac{md^2}{2I} (C_{m_q} + C_{m_{\dot{\alpha}}})_{\alpha^2} \right) \right)$$

It is seen from the Figure (4.3) and (4.4) that finite amplitude oscillations are possible only when  $\xi_1 < 0$ . These bifurcation diagrams show that limit cycle appearance and disappearance in the system is due to the variation of  $\mu$ . In Figure (4.4) it can be seen that when

$\mu < 0$  the amplitude of equilibria is unstable but after crossing  $\mu = 0$  the amplitude of equilibria become stable and a limit cycle is obtained.

#### 4.5 Solution of Amplitude and Phase-Correction Equations

To obtain a closed-form solution, it is required to solve the amplitude and phase-correction equations i.e. Equation (4.9). Recall the amplitude differential equation first, moreover using separation of variables technique, equation can be written as:

$$d\tau_1 = \frac{dA}{A(\xi_1 A^2 + \frac{\mu}{2})} \quad (4.11)$$

Carrying out partial fraction expansion, we have:

$$d\tau_1 = \frac{2}{\mu A} dA - \frac{2\xi_1 A}{(\mu\xi_1 A^2 + \frac{\mu^2}{2})} dA \quad (4.12)$$

Integrating on both sides of Equation (4.12), we have:

$$\tau_1 = \frac{2}{\mu} \ln|A| - \frac{1}{\mu} \ln \left| \mu\xi_1 A^2 + \frac{\mu^2}{2} \right| + S_0 \quad (4.13)$$

By taking exponential and simplifying further, we have:

$$\exp(\mu\tau_1) = \frac{A^2 \exp(S_0)}{\mu\xi_1 A^2 + \frac{\mu^2}{2}} \quad (4.14)$$

Rearranging the Equation (4.14),

$$A^2 = - \frac{\frac{\mu^2}{2} A^2 \exp(\mu\tau_1)}{\exp(S_0) + \mu\xi_1^2 \exp(\mu\tau_1)} \quad (4.15)$$

By letting  $S_1 = \sqrt{\frac{\mu}{\exp(S_0)}}$ , Equation (4.15) can be written as:

$$A = \frac{\sqrt{\frac{S_1 \mu}{2} \exp\left(\frac{\mu\tau_1}{2}\right)}}{\sqrt{1 - S_1 \xi_1 \exp(\mu\tau_1)}} \quad (4.16)$$

The constant  $S_1$  in above Equation (4.16) can be determined with the help of initial conditions. Furthermore, the steady state solution in Equation (4.16) matches with Equation (4.10). Now, substituting Equation (4.16) into the phase-correction equation, we get:

$$dB = \left( \frac{\frac{S_1 \mu}{2} \xi_2 \exp(\mu \tau_1)}{1 - S_1 \xi_1 \exp(\mu \tau_1)} \right) \quad (4.17)$$

Integrating on both sides of Equation (4.17), we get:

$$B = -\frac{\xi_2}{\xi_1} \ln |1 - S_1 \xi_1 \exp(\mu \tau_1)| + S_2^* \quad (4.18)$$

where,  $S_2^* = \ln |S_2|$ , is a constant. Now putting the Equation (4.16) and Equation (4.18) in Equation (4.5), we get:

$$\alpha_0 = \left( \frac{\frac{\sqrt{S_1 \mu}}{2} \exp\left(\frac{\mu \tau_1}{2}\right)}{\sqrt{1 - S_1 \xi_1 \exp(\mu \tau_1)}} \right) \sin \left( \sqrt{\left( -\frac{\rho V^2 S d}{2l} C_{m\alpha,0} \right) \tau_0 + \left( -\frac{\xi_2}{\xi_1} \ln |1 - S_1 \xi_1 \exp(\mu \tau_1)| + S_2^* \right)} \right) \quad (4.19)$$

## 4.6 Concluding Remarks

The technique Multiple Time Scales is successfully applied to Equation (3.12), an analytical approach is utilized to approximate the closed-form solution. In the next chapter the numerical validation is performed.

## Chapter 5

# NUMERICAL VALIDATION

---

### 5.1 Introduction

The closed-form solution was obtained for the oscillations of the decelerating blunt probe using MTS technique in the previous chapter. In this chapter the application of numerical validation will be carried out. A simulation of oscillations of the decelerating blunt body entry vehicle at the time of atmospheric entry was performed. The results obtained from this simulation are compared with the analytical solution developed earlier.

### 5.2 Numerical Solution

Our need is to solve Equation (4.12) numerically. For this purpose MATLAB® ordinary differential equation solver *ode45* is used to integrate the governing equations i.e. Equation (3.12). This solver is based on fourth-order Runge-Kutta method. Before we apply *ode45* technique, we need two initial conditions, as the differential equation is second order ODE.

$$\alpha_0(t = 0) = 13^\circ \quad (6.1a)$$

$$\dot{\alpha}_0(t = 0) = 0 \text{ rad/s} \quad (6.1b)$$

The model properties are taken from the experimental work of the Schoenenberger and Queen [9]:

$$m = 0.584 \text{ kg} \quad (6.2a)$$

$$I = 1.55 \times 10^{-4} \text{ km} \cdot \text{m}^2 \quad (6.2b)$$

$$V = 0.584 \text{ m/s} \quad (6.2c)$$

$$d = 0.07 \text{ m} \quad (6.2d)$$

$$S = 0.00385 \text{ m}^2 \quad (6.2e)$$

$$\rho = 1.20 \text{ kg/m}^3 \quad (6.2f)$$

$$C_{m^3} = 0.0206 \quad (6.2g)$$

$$C_{m^2} = 0.0776 \quad (6.2h)$$

$$C_{m_{\alpha,0}} = 0.1619 \quad (6.2i)$$

$$C_{l^3} = 0.925 \quad (6.2j)$$

$$C_{l^2} = -2.84 \quad (6.2k)$$

$$C_{l_{\alpha,0}} = 2.15 \quad (6.2l)$$

$$\left(C_{m_q} + C_{m_{\alpha}}\right)_{\alpha^2} = -7.6816 \quad (6.2m)$$

$$\left(C_{m_q} + C_{m_{\alpha}}\right)_{\alpha} = -0.1578 \quad (6.2n)$$

$$\left(C_{m_q} + C_{m_{\alpha}}\right)_0 = 0.3804 \quad (6.2o)$$

$$S_0 = 9.976083 \quad (6.2p)$$

$$S_2 = 3.8 \quad (6.2q)$$

### 5.3 Comparison of Analytical Solution with Numerical Simulations

It can be recognized in Figure 5.1 that the limit cycle amplitude and frequency concluded by the MTS method are in decent arrangement with numerical simulation.

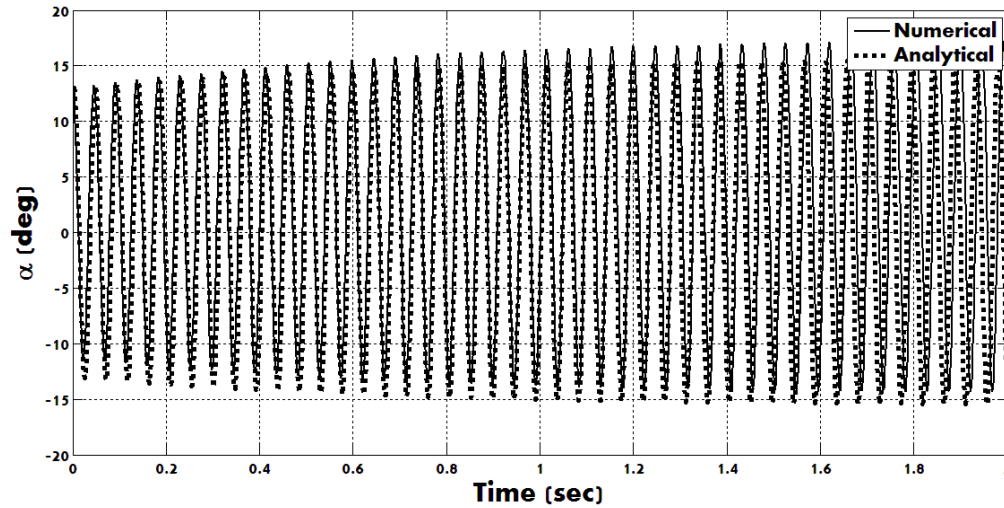


Figure 5.1 Comparison of Analytical And Numerical Solution for the Limit Cycle Case

### 5.4 Concluding Remarks

RK-4 method is utilized in MATLAB® to validate approximate closed-form solution. A satisfactory agreement with analytical solution is obtained.

## Chapter 6

# CONCLUSIONS

---

### 6.1 Introduction

This chapter includes the conclusions drawn from this research. Moreover, recommendations for future work are also listed.

### 6.2 Conclusions

The phenomenon of dynamic stability in blunt-body atmospheric entry vehicles is among the least understood. This work describes the stability analysis of a generic blunt body atmospheric entry vehicle in low supersonic regime, just before the parachute deployment. This work presents an approximate analysis that provides the amplitude of limit cycle in terms of nonlinearities associated with aerodynamic coefficients. The driving forces for oscillation growth are the cubic nonlinearities associated with the lift-curve slope and quadratic nonlinearity associated with pitch damping characteristic curve.

The analytical findings are validated with numerical simulations based on Runge-Kutta methods. A decent agreement between approximate closed-form analytical solutions and numerical results is demonstrated.

## REFERENCES

1. Allen, H.J.a.E., Jr., A. J., *A Study of the Motion and Aerodynamic Heating of Ballistic Missiles Entering the Earth's Atmosphere at High Supersonic Speeds* NACA TN 4047 (NASA Technical Report), 1957.
2. <http://dayton.hq.nasa.gov/IMAGES/LARGE/GPN-2000-001938.jpg>. 2000.
3. Gary, T.C., Leslie. and A. Yates., *Limit Cycle Analysis of Planetary Probes*. AIAA 99-1022, 1999. Reno.
4. Baillion., M., *Blunt Bodies Dynamics Derivatives*. AGARD-R-808-Capsule Aerothermodynamics, 1995.
5. <http://en.wikipedia.org/wiki/Rehbar-1>.
6. <http://en.wikipedia.org/wiki/Badr-1>. 1990.
7. [http://en.wikipedia.org/wiki/Space\\_programme\\_2040](http://en.wikipedia.org/wiki/Space_programme_2040). 2011.
8. <http://mars.jpl.nasa.gov/msp98/lander/edl1.gif>.
9. Mark, S.A.E., M. Queen., *Limit Cycle Analysis Applied to the Oscillations of Decelerating Blunt-Body Entry Vehicles*. RTO-MPAVT-152, 2008.
10. Kazemba, C.D., et al., *Survey of Blunt Body Dynamic Stability in Supersonic Flow*, in *AIAA Atmospheric Flight Mechanics Conference*. 2012, AIAA: Minnesota, USA.
11. Ramnath, R.V. and G. Sandri, *A Generalized Multiple Scales Approach to a Class of Linear Differential Equations*. *Journal of Mathematical Analysis and Applications*, 1969. 28.
12. Ramnath, R.V., *Multiple Scales Theory and Aerospace Applications*. 2010: AIAA.
13. Go, T.H. and R.V. Ramnath, *Analysis of the Two-Degree-of-Freedom Wing Rock in Advanced Aircraft*. *Journal of Guidance, Control and Dynamics*, 2002. 25(2).



14. Go, T.H., *Lateral-Directional Aircraft Dynamics Under Static Moment Nonlinearity*. Journal of Guidance, Control and Dynamics, 2009. 32(1): p. 305-309.
15. Go, T.H. and F.A.P. Lie, *Analysis of Wing Rock Due to Rolling-Moment Hysteresis*. Journal of Guidance, Control and Dynamics, 2008. 31(4): p. 849-857.
16. Tiau Hiong, G. and R.V. Ramnath, *Analytical Theory of Three-Degree-of-Freedom Aircraft Wing Rock*. Journal of Guidance, Control and Dynamics, 2004. 27(4): p. 657-664.
17. Maqsood, A. and G. Tiau Hiong, *Multiple time scale analysis of aircraft longitudinal dynamics with aerodynamic vectoring*. Nonlinear Dynamics, 2012. 69(3): p. 731-742.
18. Karen, L.B., Eric, L. Walker., Gregory, J. Brauckmann. and Philip, E. Robinson., *Development of the Orion Crew Module Static Aerodynamic Database, Part II: Supersonic / Subsonic*. AIAA 2011-3507, Jun. 2011.
19. Gary, T.C., Wayne, H. Hathaway and A. Mitcheltree., *Transonic and Low Supersonic Static and Dynamic Aerodynamic Characteristics of the Stardust Simple Return Capsule*. AIAA 1999-1021, 1999.
20. R, H.P.a.P.J., *Angle-of-Attack Motion of a Spinning Entry Vehicle*. Journal of Spacecraft and Rockets, Jan. 1969. 6.
21. Jaffe., P., *Dynamic Stability Tests of Spinning Entry Bodies in the Terminal Regime*. Journal of Spacecraft and Rockets, Jun. 1971. 8.
22. H, S.F.W., D. Wolhart, *Damping In Pitch and Static Stability of Supersonic Impact Nose Cones, Short Blunt Subsonic Impact Nose Cones, and Manned Reentry Capsules at Mach Numbers From 1.93 to 3.05*. NASA TM X-37, Nov. 1960.
23. H, S.F.a.W., D. Wolhart, *Damping in Pitch and Static Stability of a Group of Blunt Bodies from  $M=0.6$  to  $0.95$* . NASA TM X-194, 1959.

24. L, E.E., *Effect of boundary-layer transition on vehicle dynamics*. Journal of Spacecraft and Rockets, Dec. 1969. 6: p. 1402-1409.
25. Teramoto, K.F.a.K.H., *Numerical Analysis of Dynamic Stability of a Reentry Capsule at Transonic Speeds*. AIAA 98-4451, 2001. 39.
26. H, G.W., R, A. Kilgore. and E, R. Hillje., *Dynamic Directional Stability for a Group of Blunt Reentry Bodies at Transonic Speeds*. NASA TM X-337, 1960.
27. L, E.E.a.J., P. Reding., *Re-Entry Capsule Dynamics*. Journal of Spacecraft and Rockets, 1971. 8.
28. Cole, D.K., Robert, D. Braun., Ian, G. Clark. and Mark Schoeneberger., *Survey of Blunt Body Dynamic Stability in Supersonic Flow*. AIAA 2012-4509, 2012.
29. D, A.B.a.N., S. Johnson., *An Experimental and Analytical Investigation of Dynamics of Two Blunt Bodies at Supersonic Speeds*. NASA TM X-18, 1959.
30. B, H.B.a.E., C. Hedstrom., *Damping in Pitch of Bluff Bodies of Revolution at Mach Numbers from 2.5 to 3.5*. NASA TM X-90, Nov. 1959.
31. Smith., B., *Oscillation of Supersonic Inflatable Aerodynamic Decelerators at Mars*. 2010, Georgia Institute of Technology.
32. A, L.R.a.G., T. Chapman., *A Study of Reynolds Number Effects on Supersonic Flow Over Blunt Bodies*. AIAA 2000-1010, 2000.
33. D, B.O.a.V., V. Aubuchon., *Overview of Orion Crew Module and Launch Abort Vehicle Dynamic Stability*. AIAA 2011-3504, 2011.
34. Nayfeh, A.H., *Perturbation Methods*. Weinheim. 2004, Germany: Wiley-VCH Verlag GmbH & Co. KGaA.
35. Nayfeh, A.H., *Applied Nonlinear Dynamics: Analytical, Computational and Experimental Methods*. 1995, New York: Wiley.
36. Nayfeh, A.H., *Problems in Perturbation*. 1985, New York: Wiley.

37. Nayfeh, A.H., *Introduction to Perturbation Techniques*. 1981, New York: Wiley.
38. Rudrapatna, V.R., *Multiple Scales Theory and Aerospace Applications*. 2010: AIAA Education Series, ed. J.A. Schetz. 2010: American Institute of Aeronautics and Astronautics, Inc.
39. Tiau, H.G.A.R., V. Ramnath., *An Analytical Approach to the Aircraft Wing Rock Dynamics*. AIAA 2001-4426, 2001.
40. Poincaré., H., *Les Méthodes. and Nouvelles de la., Mécanique Céleste*, Gauthier-Villars, Paris. Dover, New York, 1892-1899.
41. Maqsood, A.a.T.H.G., *Multiple Time Scales Analysis of Aircraft Longitudinal Dynamics with Aerodynamic Vectoring*. Springer Nonlinear Dynamics 2012. 69: p. 731-742.
42. Steven, H.S., *Nonlinear Dynamics and Chaos*. Dec. 2000: Wesview Press.

## Appendix A

### MATLAB Codes of Analytical and Numerical Solutions

#### I. Numerical Solution

##### (i) M-File-1

```
function xp=nv(t,x)
rho=1.2;
v=343;
i=0.000155;
d=0.07;
m=0.584;
s=0.00385;

%% Aerodynamic Coefficients %%
cmx3(1)=0.0206; %AIAA M-2.5
cmx2(1)=0.0776; %AIAA M-2.5
cmx0(1)=-0.1619; %AIAA M-2.5
clx3(1)=0.925; %AIAA M-2.5
clx2(1)=-2.84; %AIAA M-2.5
clx0(1)=2.15; %AIAA% M-2.5

% DAMPING MACH# 2.5 %%
cmqcmx2(1)=-7.6816; %CMqCAlpha-M-2.5
cmqcmx1(1)=-0.1578; %CMqCAlpha-M-2.5
cmqcmx0(1)=0.3804; %CMqCAlpha-M-2.5

%% Dynamic Coefficients %%
omega2=-((rho*(v^2)*s*d)/(2*i))*(cmx0(1));
```

```

mu=((rho*v*s)/(2*m))*(-clx0(1)+((m*(d^2))/(2*i))*cmqcmx0(1));
c1=((rho*(v^2)*s*d)/i)*cmx2(1);
c2=((3*rho*(v^2)*s*d)/(2*i))*(cmx3(1));
c3=((rho*v*s)/(2*m))*(-2*clx2(1)+(m*(d^2)/(2*i))*cmqcmx1(1));
c4=(rho*v*s/(2*m))*(-3*clx3(1)+(m*(d^2)/(2*i))*cmqcmx2(1));

%% System of ODEs %%

xp=zeros(2,1);

xp(1)=x(2);

xp(2)=-
(omega2)*x(1)+mu*xp(1)+c1*(x(1).^2)+c2*(x(1).^3)+c3*x(1).*xp(1)+c4*(x(1).^2).*xp(1);

end;

```

## (ii) M-File-2

```

function readnv()
[T,Y] = ode45('nv',[0 2],[0.227 0]);
% [t,x]=ode45('F',[t0,tf],[x10,x20])
plot(T,Y(:,1)*180/pi,'-');
grid on;

```

## II. Numerical Solution

```

rho=1.2;
v=343;
i=0.000155;
d=0.07;
m=0.584;
s=0.00385;

%% Aerodynamic Coefficients %%

% AIAA MACH# 2.5 %%

cmx3(1)=0.0206; % AIAA M-2.5

```

```

cmx2(1)=0.0776; %AIAA M-2.5
cmx0(1)=-0.1619; %AIAA M-2.5
clx3(1)=0.925; %AIAA M-2.5
clx2(1)=-2.84; %AIAA M-2.5
clx0(1)=2.15; %AIAA% M-2.5

% DAMPING MACH# 2.5 %%

cmqcmx2(1)=-7.6816; %CMqCMalpha-M-2.5
cmqcmx1(1)=-0.1578; %CMqCMalpha-M-2.5
cmqcmx0(1)=0.3804; %CMqCMalpha-M-2.5

%% Dynamic Coefficients %%
c4=((rho*v*s)/(2*m)*(((3*clx3(1))+(m*(d^2)/(2*i))*(cmqcmx2(1)))));
% c4=-100;
c2=((3*rho*(v^2)*d*s)/(2*i))*(cmx3(1));
omega=-((rho*(v^2)*d*s)/(2*i))*(cmx0(1))^0.5;
exi1=(c4/8);
exi2=-(3/8)*(c2/omega);
mu=(rho*v*s/(2*m))*((-clx0(1))+((m*(d^2))/(2*i))*cmqcmx0(1));
s0= 9.976083;
s1=((mu)/exp(s0))^0.5;
s2=3.8;
epsilon=0.42;
tau=0:0.003349:4.76;
t=epsilon*tau;

%% Closed Form Solution %%
a((((s1*mu)/2)^0.5)*exp((mu*t)/2))./((1-(s1*exi1*exp(mu*t)))^0.5);
b=-(exi2/(2*exi1))*log(1-s1*exi1*exp(mu*t)) + log(s2);

```

```

% alpha0((((s1*mu)/2)^(0.5))*exp((mu*t)/2))./((1-
(s1*exi1*exp(mu*t)).^0.5)).*sin((omega*t)+(-(exi2/(2*exi1))*log((1-(s1*exi1*exp(mu*t))) +
log(s2))));

alpha0 = a.*sin(omega*t + b);

plot(t,(alpha0)*(180/pi),':');

end;

```